(10)

RESEARCH LABORATORIES

UNITED AIRCRAFT CORPORATION

UAC RESEARCH

COPY NO. 63

UNITED AIRCRAFT CORPORATION
RESEARCH LABORATORIES
EAST HARTFORD, CONN.

Report M-1492-1

Methods for Calculating Radiant Heat Transfer in High-Temperature Hydrogen Gas

Contract AF 04(611)-7448

REPORTED BY Richard W. Patch
Richard W. Patch

APPROVED BY M. Schweiger
M. Schweiger
Head, Propulsion Section

NO. OF PAGES 32

DATE November 1961

FOREWORD

Contract AF 04(611)-7448 between the Air Force Flight Test Center, Edwards Air Force Base, California, Air Force Systems Command, United States Air Force and the Research Laboratories of United Aircraft Corporation pertains to investigations of the characteristics of a unique gaseous-core nuclear rocket concept. These investigations, which were directed toward the development of information pertinent to the evaluation of the feasibility of this concept, include the following: (1) experimental determination of the characteristics of vortex flow, (2) design and fabrication of equipment to provide a radial temperature gradient in a vortex flow, (3) theoretical calculations of the characteristics of the end-wall boundary layer in a vortex tube, and (4) theoretical calculations of radiant heat transfer in the proposed engine.

The work accomplished under the contract is summarized in the following Research Laboratories' reports which comprise the required Final Report

I. Summary Report (Report R-2494-4)

II. Experimental Investigation of Characteristics of Confined Jet-Driven Vortex Flows (Report R-2494-2)

III Heat Transfer to Confined Vortex Flows by Means of a Radio-Frequency Gas Discharge (Report R-2494-3)

IV. Theoretical Solutions for the Secondary Flow on the End Wall of a Vortex Tube (Report R-2494-1)

V Methods for Calculating Radiant Heat Transfer in High-Temperature Hydrogen Gas (Report M-1492-1, Present Report)

Report M-1492-1

Methods for Calculating Radiant Heat Transfer in High-Temperature Hydrogen Gas

Contract AF 04(611)-7448

SUMMARY

A digital computer program was developed to determine heat transfer by thermal radiation in any gas with one-dimensional or axisymmetric temperature and pressure distributions. Heat transfer was calculated for a one-dimensional case with two black-body boundaries and a monotonically increasing temperature. The calculations were made with hydrogen throughout the space between the boundaries and with a grey gas added to the hydrogen at the high-temperature end. Conclusions are as follows:

This work was initiated under the Research Laboratories' own research program and completed as part of Contract AF 04(611)-7448 with the Air Force Flight Test Center, Edwards Air Force Base, California, Air Force Systems Command, United States Air Force.

CONCLUSIONS

(1) In gases the radiant heat flux densities determined by a diffusion analysis may be in error by several orders of magnitude for cases having steep temperature gradients and low absorption coefficients.

(2) Accurate values of radiant heat flux density can be obtained for all cases by employing a transport analysis and using sufficiently small increments in the numerical integration procedure.

(3) The use of a diffusion analysis for calculations where the absorption coefficient is high and a transport analysis where the absorption coefficient is low is the most practical method of solution for a general digital computer program.

(4) The bound-free absorption of the H^- ion is the most important contributor to the absorption coefficient of hydrogen at 100 atm between 7,000 K and 12,000 K.

INTRODUCTION

Quantitative data on heat transfer by thermal radiation are required in designing high-performance propulsion systems, electric arcs, and hydrogen fusion experiments because thermal radiation is an important mechanism of energy transfer at high temperatures. There have been many studies pertaining to radiant heat transfer reported in the literature but the limitations of each study preclude their use in systematic calculations for many practical cases. For example, the emissivity of hydrogen (which is of particular interest in propulsion systems due to its low molecular weight) has been calculated in Ref. 1 for temperatures up to 10,000 K, and the continuous emission of a thin layer of hydrogen for a range of temperatures up to 16,800 K has been calculated in Ref. 2. Although the latter values may be readily converted to emissivity, this quantity is useful only in cases involving layers of gas at a constant temperature.

In a diffusion analysis, the Rosseland mean opacity and the temperature gradient are used to calculate heat flux density. The Rosseland mean opacity of hydrogen has been calculated in Ref. 3 for temperatures between 6300 and 50,400 K, neglecting the important contributions due to H^- bound-free absorption and H free-free absorption. Unfortunately, as pointed out in Chapter V of Ref. 4 and proved later in this report, a diffusion analysis is not applicable to gases with low absorption coefficients and steep temperature gradients.

One-dimensional transport analyses of thermal radiation in a gas or other semi-opaque media are given in Refs. 5 and 6. Neither reference contains values for hydrogen. Reference 7 contains a one-dimensional transport analysis for pure hydrogen. However, only the heat flux reaching a wall is considered, and the extension of the bound-free H continuum to lower wave numbers due to the lowering of the ionization potential at high free-electron densities (Ref. 8) is neglected. The change in composition due to lowering of the ionization potential is also apparently neglected, and a less accurate cutoff is used for H states than in Ref. 8. A general transport analysis of thermal radiation in a gas is given in Ref. 9. The equations developed in this reference have not been applied to hydrogen, and their solution is much more complicated than the equations for a one-dimensional transport analysis.

The study described herein was initiated to provide a generalized digital computer program for use in calculating values of heat flux density and net energy loss for any gas having one-dimensional or axisymmetric temperature and pressure distributions. In developing this program specialized subroutines were provided to expedite calculations for hydrogen.

ANALYSIS

Basic Principles

Thermal radiation is composed of photons moving in various directions with the speed of light. From a macroscopic viewpoint, it is convenient to define a spectral radiation intensity, $J_{\bar{\omega}}$. Consider a specific direction in space and an infinitesimal area, dA , with its normal at an angle θ with the direction in space (Fig. 1). Let d^4E be the energy of the thermal radiation traversing dA in a solid angle about the specific direction in space $d\Omega$, in a time dt , and in a wave number interval $d\bar{\omega}$. Then $J_{\bar{\omega}}$ is defined by the relation (Ref. 4)

$$d^4E = J_{\bar{\omega}} \cos\theta \, dA \, d\Omega \, dt \, d\bar{\omega} \tag{1}$$

so that $J_{\bar{\omega}}$ is expressed in terms of energy per unit area per steradian per unit time per unit wave number. In polar coordinates, the element of solid angle, $d\Omega$, is

$$d\Omega = \sin\theta \, d\theta \, d\phi \tag{2}$$

Consequently the net energy passing through dA per unit area per unit time is

$$F = \int_0^{\infty}\int_0^{2\pi}\int_0^{\pi} J_{\bar{\omega}} \sin\theta \cos\theta \, d\theta \, d\phi \, d\bar{\omega} \tag{3}$$

F is also known as the radiant heat flux density.

The quantity $J_{\bar{\omega}}$ is well known for a black body, and for this case is represented by $B_{\bar{\omega}}$. From (Ref. 4)

$$B_{\bar{\omega}} = \frac{2hc^2\bar{\omega}^3}{e^{\frac{hc\bar{\omega}}{kT}} - 1} \tag{4}$$

$B_{\bar{\omega}}$ is independent of the angle at which the surface of the black body is viewed.

For a gas $J_{\bar{\omega}}$ is more difficult to determine than for a black body. Neglecting discrete transitions, there are three basic processes which affect $J_{\bar{\omega}}$: (1) two particles may recombine and release their excess energy as a photon in a random direction; (2) an atom, ion, or molecule may absorb a photon; and (3) two particles in a field of photons may be induced to recombine and emit a photon in the direction that the other photons are moving. All three of these processes may also occur when a free electron comes close to an atom, ion, or molecule. In this case the free electron either loses or gains kinetic energy, and the phenomenon is called a free-free transition or, collectively, Bremsstrahlung. It is convenient to define a mean free path, $\lambda_{\bar{\omega}}$, for radiation of wave number $\bar{\omega}$. This is the distance that would be required in a uniform gas for a pencil of radiation to be reduced to $\frac{1}{e}$ of its original value if only absorption is considered and both spontaneous and induced emission are neglected. The reciprocal of $\lambda_{\bar{\omega}}$ is α . Induced emission may be thought of as negative absorption, so an effective value of α , which is designated α_t and is less than α , is (Ref. 4)

$$\alpha_t = \alpha \left[1 - e^{-\frac{hc\bar{\omega}}{kT}} \right] \tag{5}$$

It is also convenient to define an optical depth (Refs. 4 and 5) as follows:

$$T_{\bar{\omega}} = \int \alpha_t \, d S \tag{6}$$

Neglecting spontaneous emission but considering absorption and induced emission, an optical depth of one is the distance required for a pencil of radiation to be reduced to $\frac{1}{e}$ of its initial value. It can be shown (Ref. 4) that $J_{\bar{\omega}}$ at any point in a gas can be found from the relation

$$\frac{d J_{\bar{\omega}}}{d T_{\bar{\omega}}} = B_{\bar{\omega}} - J_{\bar{\omega}} \tag{7}$$

which is known as the equation of transfer and includes the effects of spontaneous emission, absorption, and induced emission. Equation (7) applies to any specific direction in space. It is rigorously valid only where radiative equilibrium exists, but its use elsewhere is merely tantamount to the customary assumption that the three Einstein coefficients are independent of radiation intensity or flux density and that local thermodynamic equilibrium exists.

Diffusion Analysis

Equation (7) can be integrated directly. The value of $J_{\bar{\omega}}$ for $T_{\bar{\omega}}$ is then

$$J_{\bar{\omega}} = e^{-T_{\bar{\omega}}} \int_{-\infty}^{T_{\bar{\omega},0}} B_{\bar{\omega}}\, e^{T_{\bar{\omega}}}\, d T_{\bar{\omega}} + C_1\, e^{-T_{\bar{\omega}}} \tag{8}$$

where C_1 is a constant of integration. It is convenient to define a new optical depth, $T_{\bar{\omega}}'$, measured backwards from $T_{\bar{\omega},0}$.

$$T_{\bar{\omega}}' \equiv T_{\bar{\omega},0} - T_{\bar{\omega}} \tag{9}$$

Consequently

$$J_{\bar{\omega}} = \int_0^{\infty} B_{\bar{\omega}}\, e^{-T_{\bar{\omega}}'}\, d T_{\bar{\omega}}' + C_1\, e^{-T_{\bar{\omega},0}} \tag{10}$$

But the location of the axes from which $T_{\bar{\omega},0}$ is measured is arbitrary, so $J_{\bar{\omega}}$ cannot depend on it. Therefore

$$J_{\bar{\omega}} = \int_0^{\infty} B_{\bar{\omega}}\, e^{-T_{\bar{\omega}}'}\, d T_{\bar{\omega}}' \tag{11}$$

$B_{\bar{\omega}}$ may be expressed as a Taylor series.

$$B_{\bar{\omega}}\left(T_{\bar{\omega}}'\right) = B_{\bar{\omega}}(0) - T_{\bar{\omega}}' \frac{d B_{\bar{\omega}}}{d T_{\bar{\omega}}'} + \ldots. \tag{12}$$

Combining Eqs. (11) and (12)

$$J_{\bar{\omega}} = B_{\bar{\omega}}(0) - \frac{d B_{\bar{\omega}}}{d T_{\bar{\omega}}'} + \ldots. \tag{13}$$

Note that

$$\frac{d B_{\bar{\omega}}}{d T_{\bar{\omega}}'} = \frac{1}{a_t} \frac{d B_{\bar{\omega}}}{d S} \tag{14}$$

Combining Eqs. (13) and (14)

$$J_{\bar{\omega}} = B_{\bar{\omega}}(0) - \frac{1}{a_t} \frac{d B_{\bar{\omega}}}{d S}\Bigg)_0 + \ldots . \tag{15}$$

where $d S$ is an infinitesimal distance in the same direction as $J_{\bar{\omega}}$. Based on Eq. (3), define a spectral heat flux density $F_{\bar{\omega}}$ in the x direction

$$F_{\bar{\omega},x} = \int_0^{2\pi} \int_0^{\pi} J_{\bar{\omega}} \sin\theta \cos\theta \, d\theta \, d\phi \tag{16}$$

Combining Eqs. (15) and (16)

$$F_{\bar{\omega},x} = 2\pi \int_0^{\pi} B_{\bar{\omega}}(0) \sin\theta \cos\theta \, d\theta - 2\pi \int_0^{\pi} \frac{1}{a_t} \frac{d B_{\bar{\omega}}}{d x} \sin\theta \cos^2\theta \, d\theta + \ldots . \tag{17}$$

$$F_{\bar{\omega},x} = \frac{-4\pi}{3 a_t} \frac{d B_{\bar{\omega}}}{d x} + \ldots . \tag{18}$$

Differentiating Eq. (4)

$$\frac{d B_{\bar{\omega}}}{d x} = \frac{2 h^2 c^3 \bar{\omega}^4 e^{-\frac{hc\bar{\omega}}{kT}}}{k T^2 \left(1 - e^{-\frac{hc\bar{\omega}}{kT}}\right)^2} \frac{d T}{d x} \tag{19}$$

Combining Eqs. (18) and (19)

$$F_{\bar{\omega},x} = \frac{8\pi h^2 c^3 \bar{\omega}^4 e^{-\frac{hc\bar{\omega}}{kT}}}{3a_t k T^2 \left(1-e^{-\frac{hc\bar{\omega}}{kT}}\right)^2} \frac{dT}{dx} + \ldots. \tag{20}$$

However, the first term in Eq. (20) is not always sufficient if steep temperature gradients are present and a_t is very small in certain regions.

One-Dimensional Transport Analysis

Rather than take additional terms in Eq. (20), it is better to obtain an exact expression for the radiant heat flux density for the one-dimensional case, with the help of Eq. (7). Instead of measuring optical depth in all directions, a normal optical depth, $T_{\bar{\omega}}''$, is measured along the x axis, so

$$T_{\bar{\omega}} = T_{\bar{\omega}}'' \sec\theta \tag{21}$$

Combining Eqs. (7) and (21)

$$\frac{dJ_{\bar{\omega}}}{dT_{\bar{\omega}}''} + \sec\theta \, J_{\bar{\omega}} = \sec\theta \, B_{\bar{\omega}} \tag{22}$$

The solution of Eq. (22) is

$$J_{\bar{\omega}} = e^{-T_{\bar{\omega}}'' \sec\theta} \int_0^{T_{\bar{\omega}}''} B_{\bar{\omega}} \sec\theta \, e^{T_{\bar{\omega}}'' \sec\theta} dT_{\bar{\omega}}'' + C_2 e^{-T_{\bar{\omega}}'' \sec\theta} \tag{23}$$

Considering the boundary conditions and redefining $T_{\bar{\omega}}''$ so that it is measured backwards from the point of interest, the intensity in an infinite gas is

$$J_{\bar{\omega}} = \int_0^{\infty} B_{\bar{\omega}} \sec\theta \, e^{-T_{\bar{\omega}}'' \sec\theta} dT_{\bar{\omega}}'' \tag{24}$$

Combining Eqs. (16) and (24)

$$F_{\bar{\omega}} = \int_0^{\pi/2} 2\pi \sin\theta^- \cos\theta^- \int_0^{\infty} B_{\bar{\omega}} \sec\theta^- e^{-T_{\bar{\omega}}''^- \sec\theta^-} dT_{\bar{\omega}}''^- d\theta^-$$

$$- \int_0^{\pi/2} 2\pi \sin\theta^+ \cos\theta^+ \int_0^{\infty} B_{\bar{\omega}} \sec\theta^+ e^{-T_{\bar{\omega}}''^+ \sec\theta^+} dT_{\bar{\omega}}''^+ d\theta^+ \qquad (25)$$

where θ^-, θ^+, $T_{\bar{\omega}}''^-$, and $T_{\bar{\omega}}''^+$ are shown in Fig. 2.

Making the substitution $y = \sec\theta$ and changing the order of integration

$$F_{\bar{\omega}} = 2\pi \int_0^{\infty} B_{\omega} \int_1^{\infty} \frac{e^{-T_{\bar{\omega}}''^- y}}{y^2} dy\, dT_{\bar{\omega}}''^- - 2\pi \int_0^{\infty} B_{\bar{\omega}} \int_1^{\infty} \frac{e^{-T_{\bar{\omega}}''^+ y}}{y^2} dy\, dT_{\bar{\omega}}''^+ \qquad (26)$$

Let

$$E_2 \equiv \int_0^{\infty} \frac{e^{-T_{\bar{\omega}}'' y}}{y^2} dy \qquad (27)$$

Combining Eqs. (26) and (27)

$$F_{\bar{\omega}} = 2\pi \int_0^{\infty} B_{\bar{\omega}} E_2\, d\, T_{\bar{\omega}}''^- - 2\pi \int_0^{\infty} B_{\bar{\omega}} E_2\, d\, T_{\bar{\omega}}''^+ \qquad (28)$$

Values of E_2 are tabulated in Ref. 10 and are plotted in Fig. 3. Physically Eq. (28) is merely the difference between the radiation from two opposite hemispheres.

In order to make Eq. (28) applicable to gases extending finite distances instead of infinite distances, it is necessary to consider boundary conditions. Assuming the boundaries are black bodies and considering absorption and induced emission, the radiation $R_{\bar{\omega}}$ at the reference point in the gas due to Boundary 1 is from Eq. (16)

$$R_{\bar{\omega}} = \int_0^{\frac{\pi}{2}} 2\pi \sin\theta^- \cos\theta^- B_{\bar{\omega}_1} e^{-T_{\bar{\omega}}''^- \sec\theta^-} d\theta^- \tag{29}$$

Substituting $y = \sec\theta$

$$R_{\bar{\omega}} = 2\pi B_{\bar{\omega}} \int_1^{\infty} \frac{e^{-T_{\bar{\omega}}''^- y}}{y^3} dy \tag{30}$$

Let

$$E_3 \equiv \int_1^{\infty} \frac{e^{-T_{\bar{\omega}}'' y}}{y^3} dy \tag{31}$$

Values of E_3 are tabulated in Ref. 10 and plotted in Fig. 3. Combining Eqs. (30) and (31)

$$R_{\bar{\omega}} = 2\pi B_{\bar{\omega}} E_3 \tag{32}$$

Considering both boundaries and combining Eqs. (28) and (32)

$$F_{\bar{\omega}} = 2\pi \int_0^{T_{\bar{\omega},1}''^-} B_{\bar{\omega}} E_2 dT_{\bar{\omega}}''^- + 2\pi B_{\bar{\omega}} E_3 - 2\pi \int_0^{T_{\bar{\omega},2}''^+} B_{\bar{\omega}} E_2 dT_{\bar{\omega}}''^+ - 2\pi B_{\bar{\omega}} E_3 \tag{33}$$

Evaluation of Eq. (33) requires numerical methods. Equations (17) and (18) of Ref. 6 are equivalent to Eq. (33)

Comparison of Diffusion and One-Dimensional Transport Analyses

Equation (33) always gives an accurate answer if the numerical analysis is carried out with sufficiently small increments. Consequently Eq. (20) can be compared with Eq. (33) to obtain an idea of the range of validity of the first term of Eq. (20). To do this, it is necessary to assume the relationship between temperature and normal optical depth. For a linear relationship, the results shown in Fig. 4 were obtained. The temperature indicated on each curve

was, of course, the temperature at the point for which the flux density was calculated. The quantity $\pi B_{\bar{\omega}}$ is the hemispherical spectral flux density from a black body. It is evident that there is a good possibility that the first term of Eq. (20) will not give an accurate answer if $F_{\bar{\omega},DIFF}/\pi B_{\bar{\omega}}$ exceeds 0.3. Unfortunately, this is not a good criterion for deciding whether or not to use Eq. (20) or (33) because the criterion is sensitive to the manner in which temperature varies with normal optical depth. In certain cases the first term of Eq. (20) may give answers that are off by two orders of magnitude.

Axisymmetric Transport Analysis

It is apparent that a diffusion analysis is not adequate for all cases likely to be encountered, while a one-dimensional transport analysis is based on a geometric assumption which is not sufficiently realistic for some propulsion systems. A rigorous axisymmetric transport analysis requires solution of the relation

$$F_{\bar{\omega}} = \int_0^{2\pi}\int_0^{\pi}\int_0^{\infty} B_{\bar{\omega}}\, e^{-T_{\bar{\omega}}'}\, dT_{\bar{\omega}}' \sin\theta\cos\theta\, d\theta\, d\phi \qquad (34)$$

which is the result of combining Eqs. (11) and (16). Solution of Eq. (34) is difficult even for a high-speed digital computer. Instead, it appears reasonable to include approximate correction factors $r/\tilde{r}$ in Eq. (33) to allow for the decrease in flux density with increasing area as radius increases. The quantity $\tilde{r}$ is the radius to which $F_{\bar{\omega}}$ applies (also the reference radius for $T_{\bar{\omega}}''$) and is shown in Fig. 5. Because the high-temperature gas near the center is frequently almost opaque and has only moderate temperature gradients, it is frequently a good approximation to replace the central portion of the gas with a black body inner wall at the same temperature, as shown in Fig. 5. With the $r/\tilde{r}$ factors, Eq. (33) becomes

$$F_{\bar{\omega}} = 2\pi \int_0^{T_{\bar{\omega},c}''} \frac{r}{\tilde{r}}\, B_{\bar{\omega}}\, E_2\, dT_{\bar{\omega}}'' + 2\pi\, \frac{r_c}{\tilde{r}}\, B_{\omega}\, E_3$$

$$- 2\pi \int_0^{T_{\bar{\omega},w}''^{+}} \frac{r}{\tilde{r}}\, B_{\bar{\omega}}\, E_2\, dT_{\bar{\omega}}''^{+} - 2\pi\, \frac{r_w}{\tilde{r}}\, B_{\bar{\omega}}\, E_3 \qquad (35)$$

Equation (35) gives a reliable result for heat flux reaching the outer wall if the gas is almost opaque out to a certain radius and then becomes transparent. This is approximately what happens in typical cases with hydrogen. However, Eq. (35) should be used with great caution, as it does not give zero flux density for a gas at uniform temperature as it should do. Also, it gives invalid answers near the center.

Over-all Flux and Net Energy Loss

To find a sufficiently accurate over-all radiant heat flux density (including radiation of all wave numbers), it is necessary to integrate the spectral heat flux density over the wave numbers where thermal radiation could possibly be appreciable at the temperatures under consideration.

$$F = \int F_{\bar{\omega}} \, d\bar{\omega} \tag{36}$$

This is applicable to either the one-dimensional or axisymmetric case.

The net energy loss, ϵ, by the gas due to spontaneous emission, induced emission, and absorption of thermal radiation of all wave numbers is

$$\epsilon = -\frac{\operatorname{div} F}{\rho} \tag{37}$$

Consequently, for the axisymmetric case

$$\epsilon = \frac{1}{r\rho} \frac{d}{dr} (rF) \tag{38}$$

The Absorption Coefficient

To determine a_ν for hydrogen, it is necessary to specify the wave number, temperature, and total pressure, and to calculate the partial pressures of H_2, e, H^+, H^-, the various states of the H atom, the ionization potentials of H^- and H, and the term values of the various states of the H atom. The method for determining these is given in Ref. 8, except for the partial pressure of H^- and its ionization potential. At pressures on the order of 100 atm and temperatures at or above 6000 K, it is permissable to assume

$$P = P_{H_2} + P_e + P_{H^+} + P_H \tag{39}$$

and solve for the partial pressures of H_2, e, H^+, and H as specified in Ref. 8. P_{H^-} is less than a tenth of P_e and less than 4×10^{-4} P, so P_{H^-} can be found to a good approximation by

$$\frac{P_H P_e}{P_{H^-}} = \frac{2\beta Q_H (2\pi m)^{\frac{3}{2}} (kT)^{\frac{5}{2}}}{h^3} e^{-\frac{hc I_{H^-}}{kT}} \tag{40}$$

where I_{H^-} is 6.048×10^3 cm^{-1} (Ref. 2). The variation of I_{H^-} with free-electron density was not considered because Ref. 1 states that the lower effective core charge of the H^- ion in the presence of free electrons produces a smaller change in ionization potential than for an atom. At 100 atm and temperatures below 6000 K, the absorption coefficient of hydrogen does not exceed 3×10^{-3} cm^{-1} below 109,000 wave numbers, so errors due to the use of Eqs. (39) and (40) have negligible effect on heat transfer for outer walls up to a meter in diameter.

There are nine continuous absorption coefficients for the species and wave numbers important for hydrogen at high temperatures. Five of these are due to H bound-free transitions where H has a principal quantum number of from 1 to 5. For low free-electron densities, the relations are given in Refs. 11 and 12. However, for high free-electron densities, the ionization potential of H is lowered as pointed out in Ref. 8, so that bound-free transitions occur at smaller wave numbers. The equations of Refs. 11 and 12 were found to give a fair approximation for these smaller wave numbers. Let a_n be the absorption coefficient (excluding induced emission) for bound-free absorption of H with principal quantum number, n, between 1 and 5. Then if $\bar{\omega} \geq I_{H^-} - \omega_n$

$$a_n = \frac{32}{3\sqrt{3}} \frac{P_{H,n} \pi^2 e^6 R_y}{\beta k T h^3 c^3 n^5 \bar{\omega}^3} \left[1 + .1728 \left(\frac{\bar{\omega}_3}{R_y} \right)^{\frac{1}{3}} - .1728 \frac{2 R_y}{\omega n^2} \left(\frac{\bar{\omega}}{R_y} \right)^{\frac{1}{3}} \right] \tag{41}$$

If $\bar{\omega} < I_H - \omega_n$

$$a_n = 0 \tag{42}$$

Let α_6 be the absorption coefficient (excluding induced emission) for free-free transitions between H^+ and a free electron. Then according to Refs. 11 and 12

$$\alpha_6 = \frac{4 R_y h^2 e^2 P_e^2}{3\sqrt{6}\,\beta^2 \pi^{\frac{3}{2}} m^{\frac{5}{2}} c^3 \bar{\omega}^3 k^{\frac{5}{2}} T^{\frac{5}{2}}} \left[1 + .1728 \left(\frac{\bar{\omega}}{R_y}\right)^{\frac{1}{3}} + .3456 \frac{kT}{hc\bar{\omega}} \left(\frac{\bar{\omega}}{R_y}\right)^{\frac{1}{3}} \right] \quad (43)$$

Let α_7 be the absorption coefficient (excluding induced emission) for free-free transitions between an H atom and a free electron. Such transitions are sometimes called H^- free-free transitions. The pseudo cross sections for such events have been evaluated and tabulated in Refs. 2 and 13 for temperatures between 2520 and 16,800 K and wave numbers between 548 and 24,690 cm^{-1}. For use in typical cases, these values were extrapolated to 40,000 K and 27,420 cm^{-1}. The pseudo cross section and α_7 are related by

$$\alpha_7 = \frac{P_e P_H \hat{\sigma}_H}{\beta^2 kT} \quad (44)$$

The bound-free absorption coefficient of H^- is represented by α_8 (excluding induced emission). The cross section for this transition is tabulated for wave numbers between 548 and 198,000 cm^{-1} in Refs. 13 and 14. The cross section and α_8 are related by

$$\alpha_8 = \frac{P_{H^-} \bar{\sigma}_{H^-}}{\beta kT} \quad (45)$$

The H_2 molecule has a dissociation continuum at wave numbers greater than 117,730 cm^{-1} (Ref. 15), and has an ionization continuum at wave numbers greater than 124,000 cm^{-1} (Ref. 16). The combined cross section in megabarns (10^{-18} cm^2) for these transitions is given in Ref. 16 as a function of wave length. The cross section and the corresponding absorption coefficient, α_9, are related by

$$\alpha_9 = \frac{P_{H_2} \bar{\sigma}_{H_2}}{\beta kT} \quad (46)$$

where $\bar{\sigma}_{H_2}$ is expressed in cm^2.

To compute a_t for hydrogen, the induced emission factor must be included. Neglecting discrete transitions

$$a_t = \sum_{n=1}^{9} a_n \left[1 - e^{-\frac{hc\omega}{kT}} \right] \tag{47}$$

It was assumed that the grey gas had a maximum absorption coefficient of 1 cm^{-1} for all wave numbers. The particle density of the grey gas was assumed to be small compared to the particle density of hydrogen, and ionization of the grey gas was neglected in computing hydrogen composition.

RESULTS

A digital computer program was developed to use either Eq. (20) or (35) to calculate spectral heat flux density. Necessary inputs when hydrogen is present include temperature and pressure at eleven equispaced radii. The program utilizes Eqs. (39) and (40) together with the procedure described in Ref. 8 to calculate composition, ionization potential of H , and term values for H . The results for 100 atm and 12,000 K are summarized in Table I. The absorption coefficients for hydrogen are then calculated by Eqs. (41) through (47) and are given in Fig. 6 for 100 atm and 12,000 K. Provision is also made to add arbitrary absorption coefficients at each of the 5 to 51 wave numbers used at the eleven radii to take into account grey gas or other gas added to the hydrogen.

If no hydrogen is present, the program may be used for any gas or combination of gases by computing their absorption coefficients independently of the program and using the sum of these absorption coefficients as inputs to the program. In this case, T must be given at eleven radii, but P is not needed.

Next, spectral heat flux density may be calculated using Eq. (20) or (35) as applicable. The program decides whether to apply Eq. (20) or (35) based on the magnitude of the total absorption coefficient, the radius increment, and two constants, which are part of the input. Use of Eq. (35) for all calculations would unduly complicate the program and increase the running time due to the large number of integration increments required if a_t is high. If it is desired to use Eq. (33) instead of Eq. (35), it is merely necessary to add a large constant to all eleven radii. Then, in Eq. (35)

$$\frac{r}{\tilde{r}} \approx 1 \qquad (48)$$

so Eq. (35) becomes Eq. (33) for all practical purposes, and a one-dimensional analysis is obtained.

When all the spectral heat flux densities have been calculated, Eq. (36) is used to obtain the over-all heat flux density. Equation (38) can then be used to obtain the net energy loss by the gas at eleven radii.

A case involving hydrogen and a grey gas was calculated based on the temperature distribution given in Fig. 7, a pressure of 100 atm, an inner wall radius of 1.524 cm, an outer wall radius of 15.24 cm, and the distribution of grey gas indicated by the absorption coefficient of the grey gas in Fig. 8. 998.476 cm was arbitrarily added to all radii to obtain a one-dimensional analysis. Equation (35) was used to obtain the spectral heat flux density if a_t was less than 44 cm^{-1}, whereas Eq. (20) was used for a_t greater than 44 cm^{-1}.

The total absorption coefficient, a_t , including the grey gas absorption coefficient, is shown in Fig. 8 for a wave number of 40,000 cm^{-1}. The heat flux density is shown in Fig. 9, together with the black-body hemispherical intensity for the temperature corresponding to the radius. The black-body hemispherical intensity is the heat flux density that a black body would radiate to cold surroundings. The heat flux density exceeds the black-body hemispherical intensity at radii greater than about 8 cm. The heat flux density reaching the outer wall is 22 percent of the inner-wall black-body hemispherical intensity. Figure 10 shows which wave numbers are important. The upper curve is the black-body spectral hemispherical intensity for the temperature of the inner wall, and the lower curve is the spectral heat flux density reaching the outer wall.

Figure 11 gives the net energy loss by the gas. It can be seen that the region of the grey gas is gaining energy from the hydrogen at small radii, whereas the hydrogen at about 7 cm is losing energy to hydrogen at greater radii and to the outer wall.

A second sample was computed without adding 998.476 cm to any radii. The heat flux density at the outer wall was found to be only 11 percent of the inner wall black-body hemispherical intensity.

ngp

REFERENCES

1. Olfe, D.: Equilibrium Emissivity Calculations for a Hydrogen Plasma at Temperatures up to 10,000 K. Technical Report No. 14, Daniel and Florence Guggenheim Jet Propulsion Center, California Institute of Technology, Pasadena, California, May 1960.

2. Mastrup, Frithjof: Continuous Emission of Hydrogen Plasmas. Journal of the Optical Society of America, Vol. 50, No. 1, January 1960.

3. Unsöld, A.: Über den Kontinuierlichen Absorptionskoeffizienten und das Spektrum einer Sternatmosphäre, welche nur aus Wasserstoff besteht. Zeitschrift für Astrophysik, Bd. 8, 1934.

4. Chandrasekhar, S.: An Introduction to the Study of Stellar Structure. Dover Publications, Incorporated, New York, 1957.

5. Pomerantz, Jacob: The Influence of the Absorption of Radiation in Shock Tube Phenomena. NAVORD Report 6136, U.S. Naval Ordnance Laboratory, White Oak, Maryland, 15 August 1958.

6. Goulard, R. and M.: One-Dimensional Energy Transfer in Radiant Media. International Journal of Heat and Mass Transfer, Vol. 1, 1960.

7. Wahl, Bruno W., J. W. McKee, and Robert J. Gould: Radiative Properties of Hydrogen and Radiative Transfer to the Environment at Elevated Temperatures. American Rocket Society Preprint 1997-61.

8. Patch, R. W.: Composition of Hydrogen Gas at High Pressures and Temperatures. UAC Research Laboratories Report UAR-0835, March 29, 1961.

9. Viskanta, Raymond: Heat Transfer in Thermal Radiation Absorbing and Scattering Media. Argonne National Laboratory, Report ANL-6170, Argonne, Illinois, May 1960.

10. Case, K. M., F. de Hoffmann, and G. Placzek: Introduction to the Theory of Neutron Diffusion, Vol. I, Report LA-NN-1, Los Alamos Scientific Laboratory, Los Alamos, New Mexico, June 1953.

11. Penner, S. S.: Quantitative Molecular Spectroscopy and Gas Emissivities. Addison-Wesley Publishing Co., Inc., Reading Massachusetts, 1959.

12. Menzel, D. H., and C. L. Pekeris: Absorption Coefficients and Hydrogen Line Intensities. Monthly Notices of the Royal Astronautical Society, Vol. 96, November 1935.

13. Chandrasekhar, S., and F. H. Breen: On the Continuous Absorption Coefficient of the Negative Hydrogen Ion. III. Astrophysical Journal, Vol. 104, 1946.

14. Chandrasekhar, S.: On the Continuous Absorption Coefficient of the Negative Hydrogen Ion. II. Astrophysical Journal, Vol. 104, 1946.

15. Dieke, G. H., and J. J. Hopfield: The Structure of the Ultra-Violet Spectrum of the Hydrogen Molecule. Physical Review, Vol. 30, October 1927.

16. Flügge, S.: Encyclopedia of Physics, Vol. 21, Springer - Verlag, Berlin, 1956.

LIST OF SYMBOLS

α	Absorption coefficient, 1/cm
A	Area, cm^2
B	Black-body intensity, erg/cm^2 ster sec
$B_{\tilde{\omega}}$	Black-body spectral intensity, erg/cm ster sec
C	Velocity of light, cm/sec
C_1	Constant of integration, erg/cm ster sec
C_2	Constant of integration, erg/cm ster sec
D	Diameter, cm
e	Charge of electron, esu; also base of natural logarithms
E	Energy, ergs
E_2	A definite integral, dimensionless
E_3	A definite integral, dimensionless
F	Radiant heat flux density, erg/cm^2 sec
$F_{\tilde{\omega}}$	Spectral radiant heat flux density, erg/cm sec
h	Plancks constant, erg sec
I	Ionization potential, cm^{-1}
$J_{\tilde{\omega}}$	Spectral radiation intensity, erg/cm ster sec
k	Boltzmann constant, erg/K
m	Mass of electron, gm
P	Pressure, atm
Q	Electronic partition function, dimensionless
r	Radius, cm

γ	Reference radius, cm
R_y	Rydberg constant for hydrogen, cm^{-1}
$R_{\bar{\omega}}$	Spectral hemispherical radiation intensity, erg/cm sec
S	Length, cm
t	Time, sec
T	Temperature, K
x	Distance along x axis, cm
y	Sec θ , dimensionless
β	Conversion factor, 9.869×10^{-7} atm cm^2/dyne
ϵ	Net energy loss by gas, erg/gr sec
θ	Angle with x axis, radians
$\lambda_{\bar{\omega}}$	Spectral mean free path for radiation, cm
ρ	Density, gr/cm^3
θ	Pseudo cross section, cm^4/dyne
$\bar{\sigma}$	Cross section, cm^2
$T_{\bar{\omega}}$	Spectral optical depth measured from fixed axes, dimensionless
$T_{\bar{\omega}}'$	Spectral optical depth measured backwards from point of interest, dimensionless
$T_{\bar{\omega}}''$	Spectral normal optical depth, dimensionless
ϕ	Azimuth angle, radians
ω	Term value, cm^{-1}
$\bar{\omega}$	Wave number, cm^{-1}
Ω	Solid angle, ster

Superscripts

$+$	In $+r$ or $+x$ direction
$-$	In $-r$ or $-x$ direction

Subscripts

c	Inner wall
DIFF	Diffusion analysis
e	Free electron
GREY	Grey gas
H	Neutral H
H^-	Negative H ion
H^+	Positive H ion
H_2	H_2 molecule
n	Principal quantum number of H
o	Reference
t	Including induced emission
TRANS	Transport analysis
w	Outer wall
x	x direction
ω	Spectral

TABLE I

Composition, Ionization Potential, and Term Values for Hydrogen at 100 atm and 12,000 K

$P_{H_2} = 3.3 \times 10^{-1}$ atm

$P_{H^-} = 1.54 \times 10^{-2}$ atm

$P_{H^+} = 1.61$ atm

$P_e = 1.61$ atm

$P_{H,\, n=1} = 9.6 \times 10^{1}$ atm

$P_{H,\, n=2} = 2.0 \times 10^{-2}$ atm

$P_{H,\, n=3} = 7.1 \times 10^{-3}$ atm

$P_{H,\, n=4} = 5.5 \times 10^{-4}$ atm

$P_{H,\, n=5} = 0$

$I_H = 1.0152 \times 10^{5}$ cm^{-1}

$\omega_1 = 0$

$\omega_2 = 8.228 \times 10^{4}$ cm^{-1}

$\omega_3 = 9.772 \times 10^{4}$ cm^{-1}

$\omega_4 = 1.0412 \times 10^{5}$ cm^{-1}

$\omega_5 = 1.1023 \times 10^{5}$ cm^{-1}

FIG. 1

COORDINATE SYSTEM AND SOLID ANGLE FOR $J_{\vec{\Omega}}$

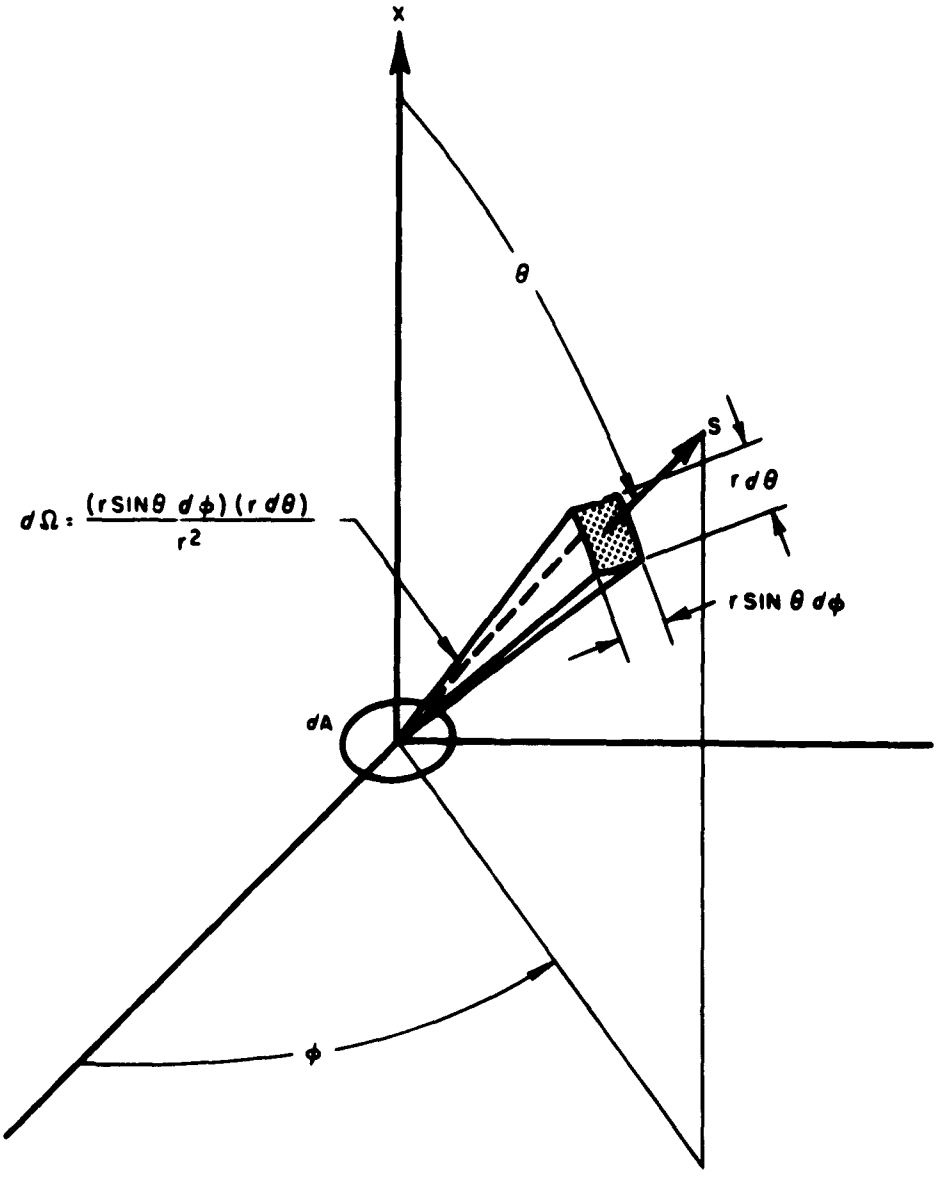

M-1492-1

FIG. 2

QUANTITIES IN A ONE-DIMENSIONAL TRANSPORT ANALYSIS

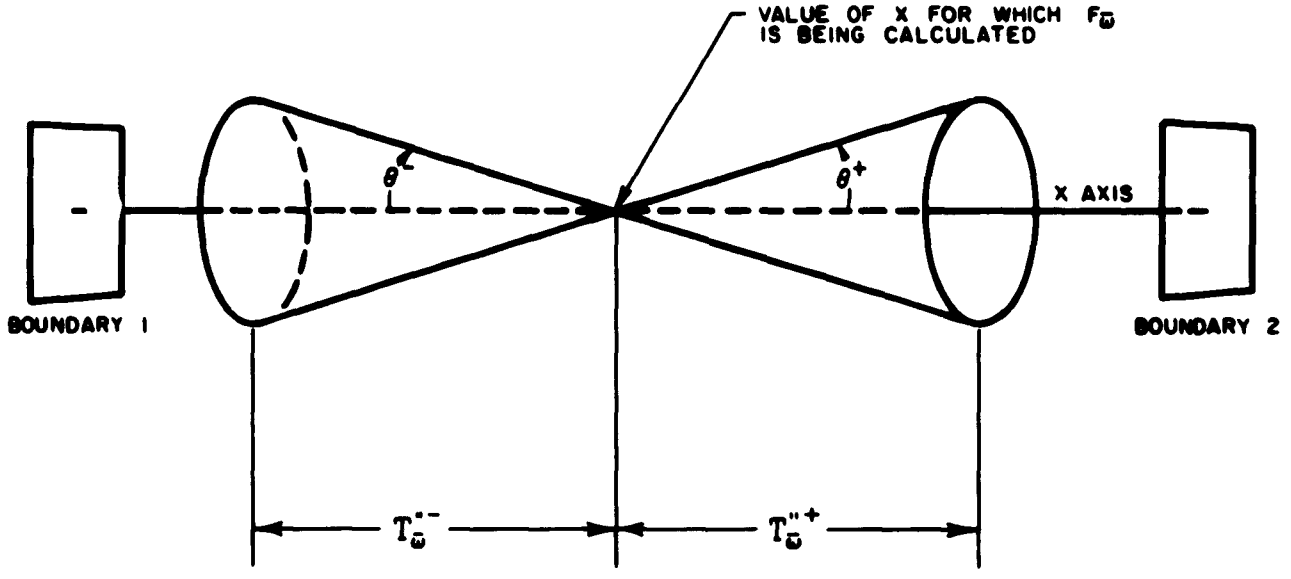

FIG. 3

VALUES FOR E_2 AND E_3

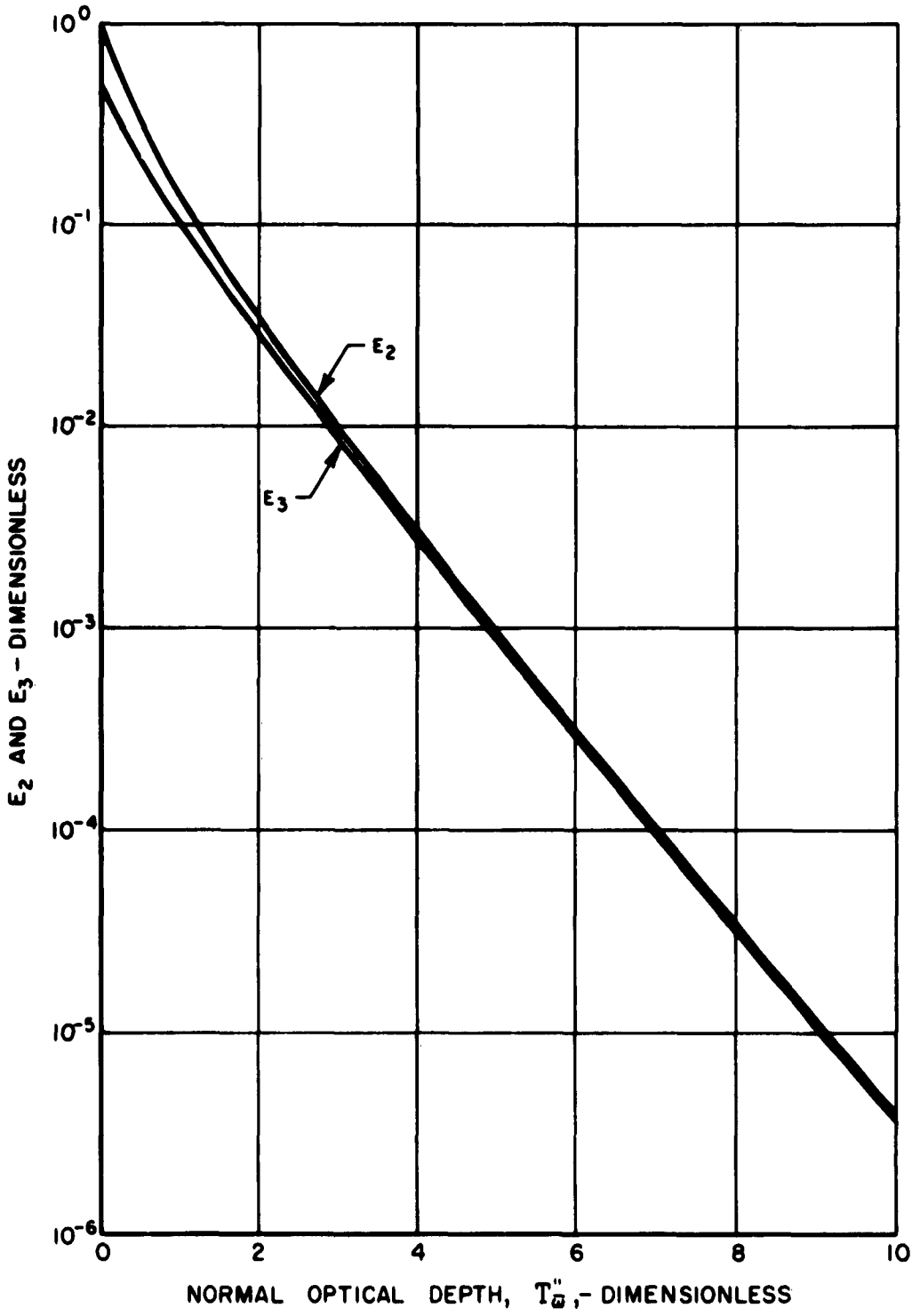

M-1492-1

FIG. 4

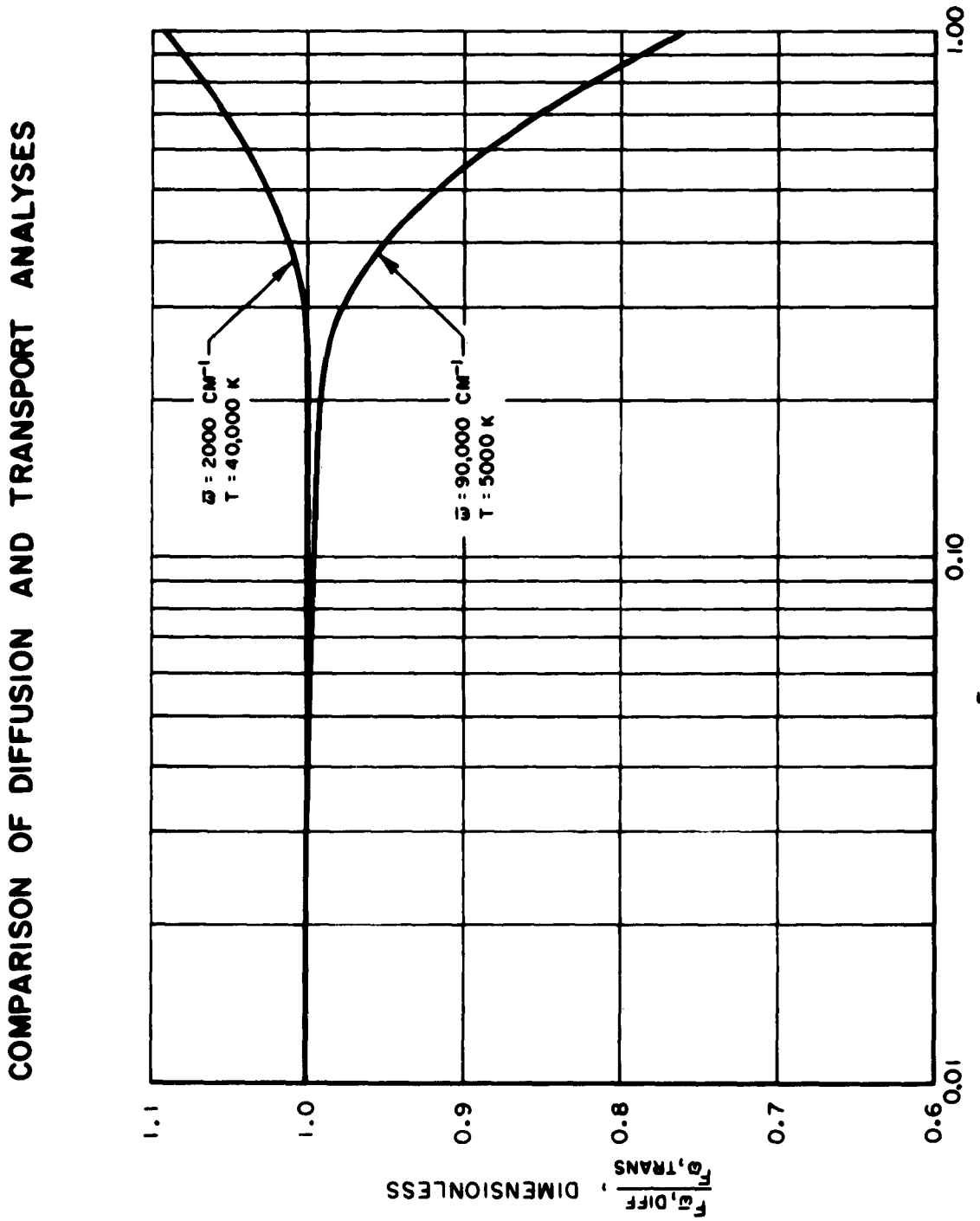
COMPARISON OF DIFFUSION AND TRANSPORT ANALYSES
$\bar{\omega}$ = 2000 CM^{-1}
T = 40,000 K
$\bar{\omega}$ = 90,000 CM^{-1}
T = 5000 K
1.1
1.0
0.9
0.8
0.7
0.6
1.00
0.10
0.01
$\frac{F_{\bar{\omega},DIFF}}{F_{\bar{\omega},TRANS}}$, DIMENSIONLESS
$\frac{F_{\bar{\omega},DIFF}}{\pi B_{\bar{\omega}}}$, DIMENSIONLESS

QUANTITIES IN AN AXISYMMETRIC TRANSPORT ANALYSIS

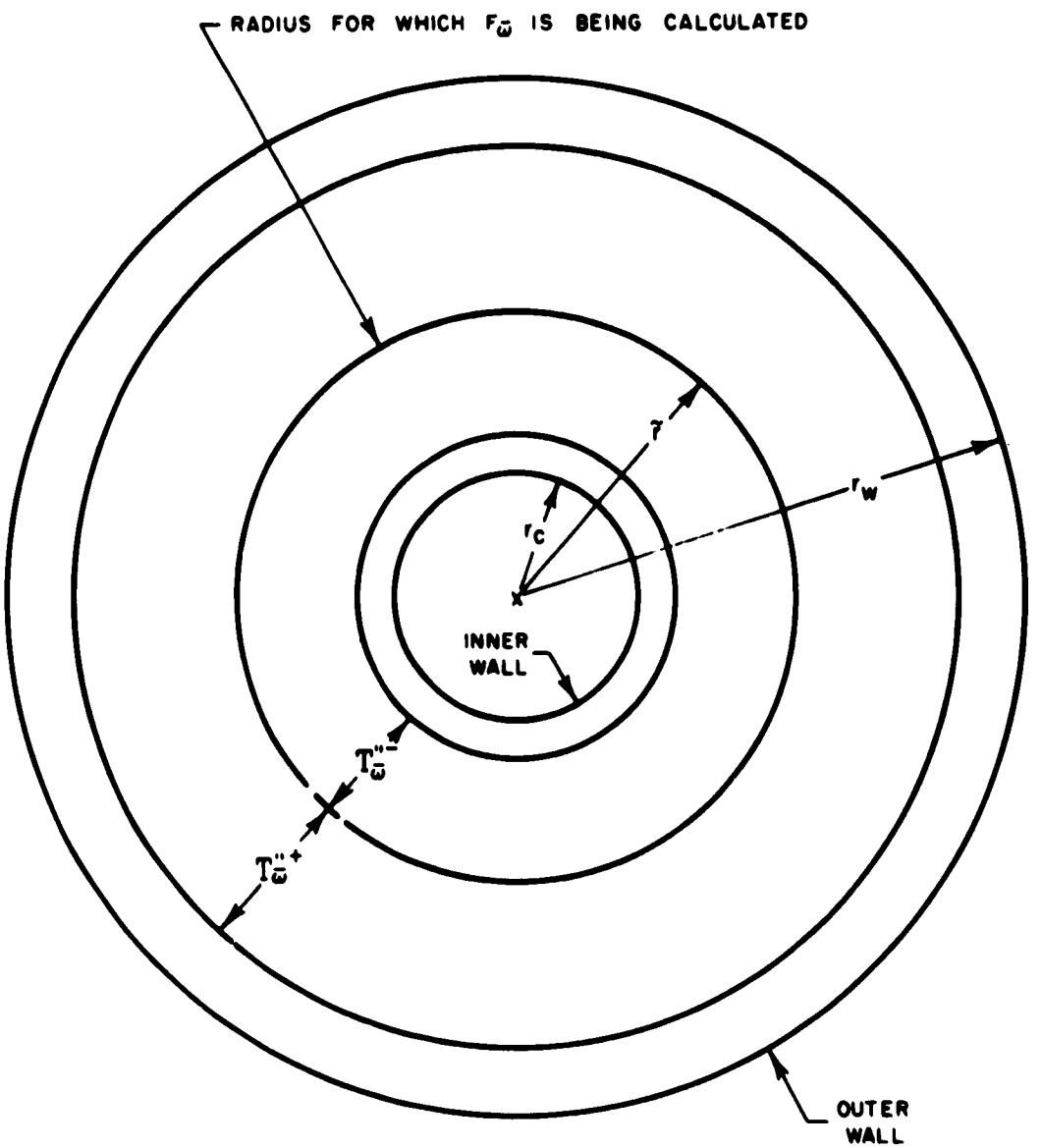

M - 1492 - 1

FIG. 6

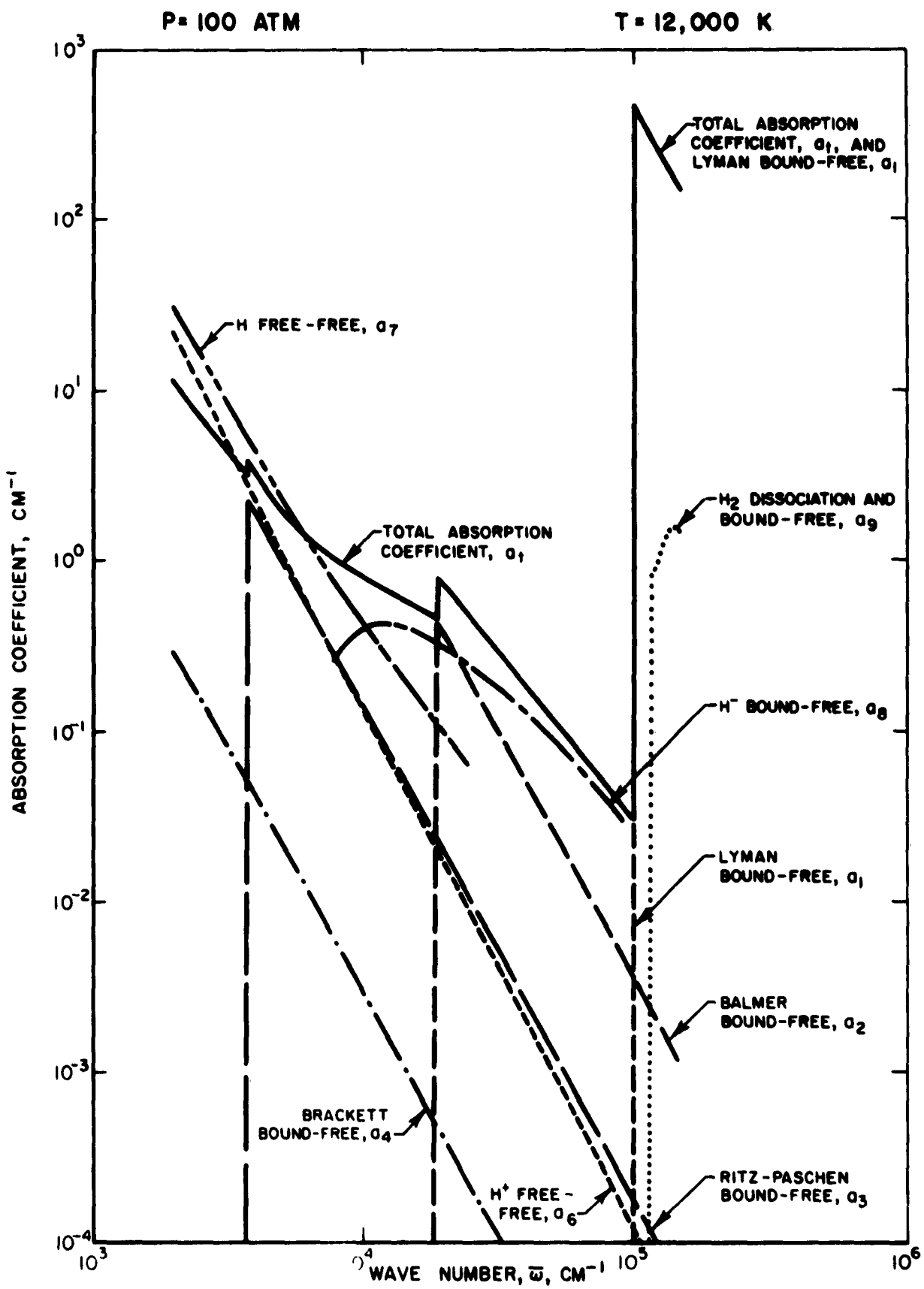
ABSORPTION COEFFICIENT FOR HYDROGEN
P = 100 ATM
T = 12,000 K
ABSORPTION COEFFICIENT, CM⁻¹
WAVE NUMBER, ω̄, CM⁻¹
TOTAL ABSORPTION COEFFICIENT, α_t, AND LYMAN BOUND-FREE, α_1
H FREE-FREE, α_7
TOTAL ABSORPTION COEFFICIENT, α_t
H₂ DISSOCIATION AND BOUND-FREE, α_9
H⁻ BOUND-FREE, α_8
LYMAN BOUND-FREE, α_1
BALMER BOUND-FREE, α_2
BRACKETT BOUND-FREE, α_4
H⁺ FREE-FREE, α_6
RITZ-PASCHEN BOUND-FREE, α_3

FIG. 7

ASSUMED TEMPERATURE FOR A TYPICAL CASE
HYDROGEN + GREY GAS

P = 100 ATM

D = 30.48 CM = 1 FT

T_C = 19,444 K = 35,000 R

T_W = 2222.2 K = 4000 R

ONE DIMENSIONAL

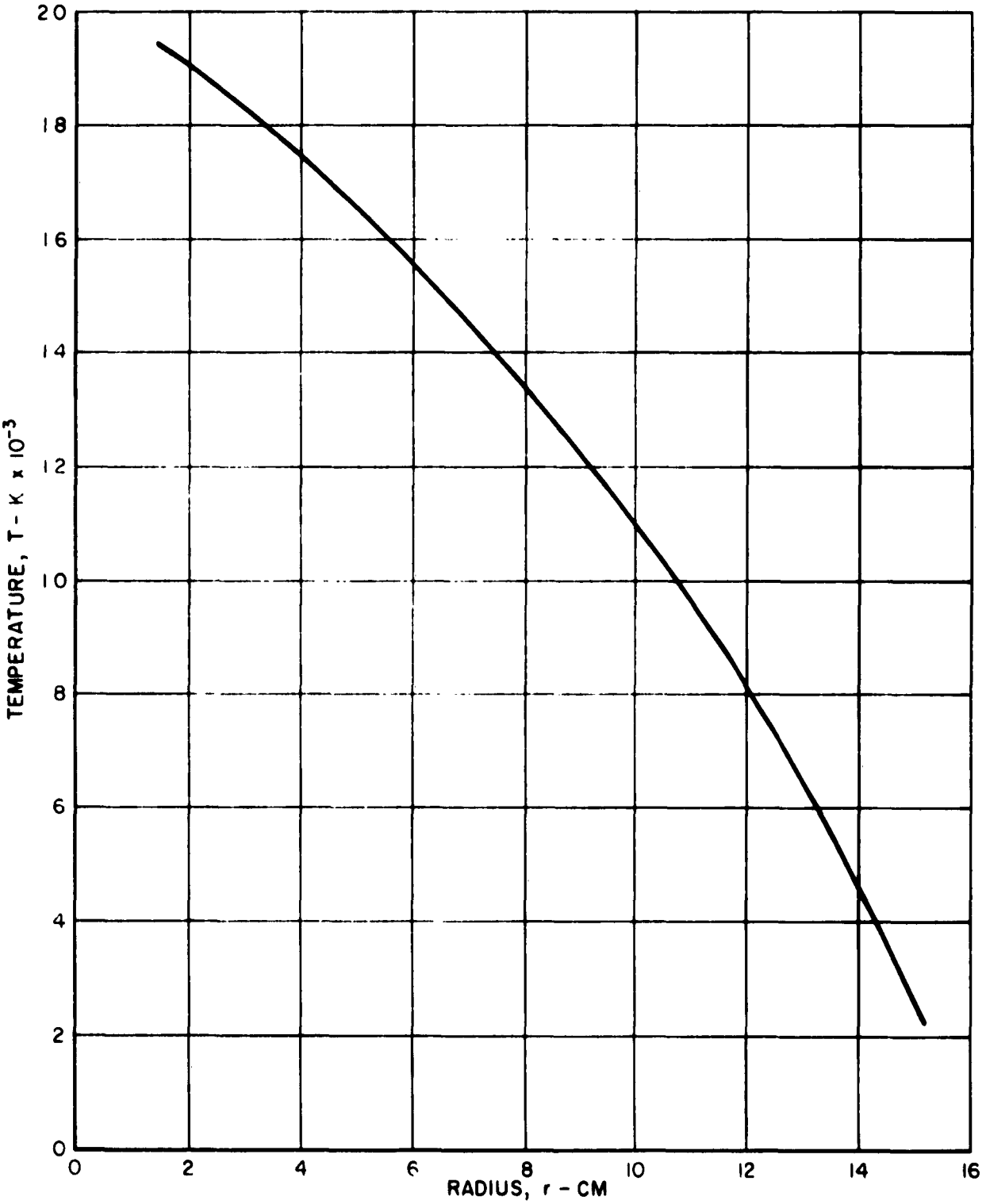

M - 1492 - 1

FIG. 8

SPECTRAL ABSORPTION COEFFICIENT FOR A TYPICAL CASE

HYDROGEN + GREY GAS

P = 100 ATM

D = 30.48 CM = 1 FT

T_C = 19,444 K = 35,000 R

T_W = 2222.2 K = 4000 R

ONE DIMENSIONAL

$\bar{\omega}$ = 40,000 CM^{-1}

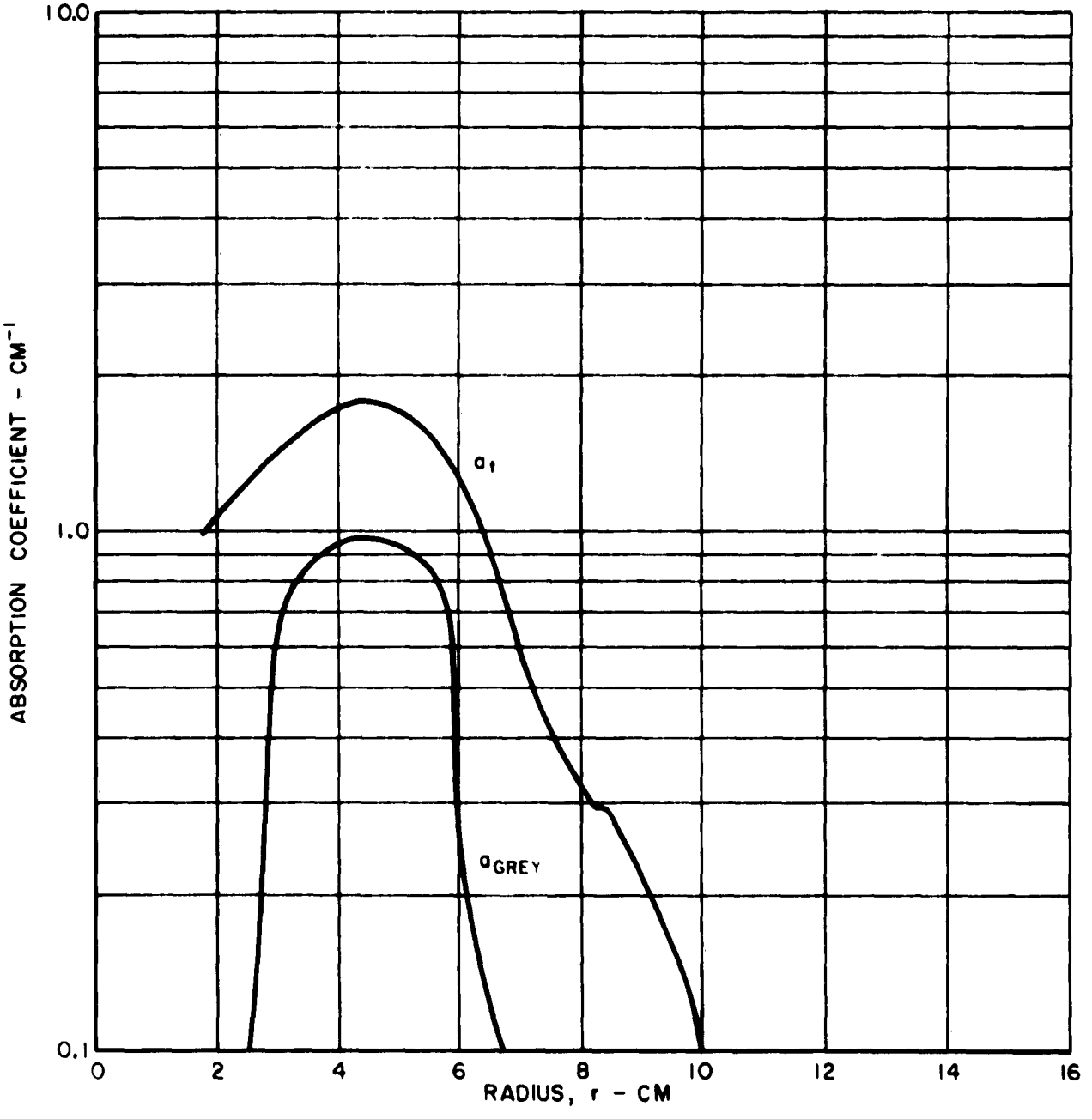

FIG. 9

HEAT FLUX DENSITY FOR A TYPICAL CASE

HYDROGEN + GREY GAS

P = 100 ATM
D = 30.48 CM = 1 FT
T_C = 19,444 K = 35,000 R
T_W = 2222.2 K = 4000 R
ONE DIMENSIONAL

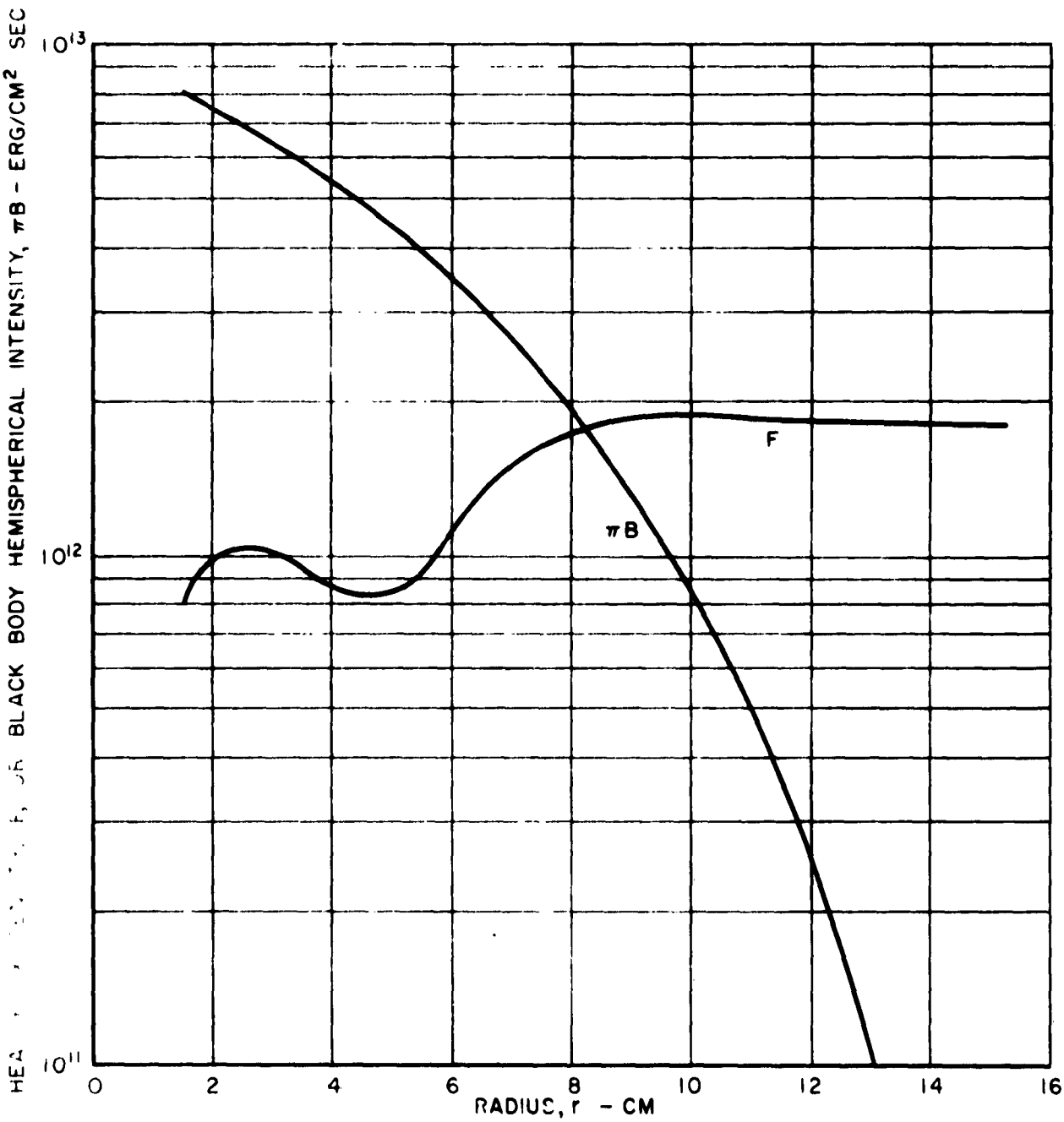

FIG. 10

SPECTRAL HEAT FLUX DENSITY FOR A TYPICAL CASE

HYDROGEN + GREY GAS

P = 100 ATM

D = 30.48 CM = 1 FT

T_C = 19,444 K = 35,000 R

T_W = 2222.2 K = 4000 R

ONE DIMENSIONAL

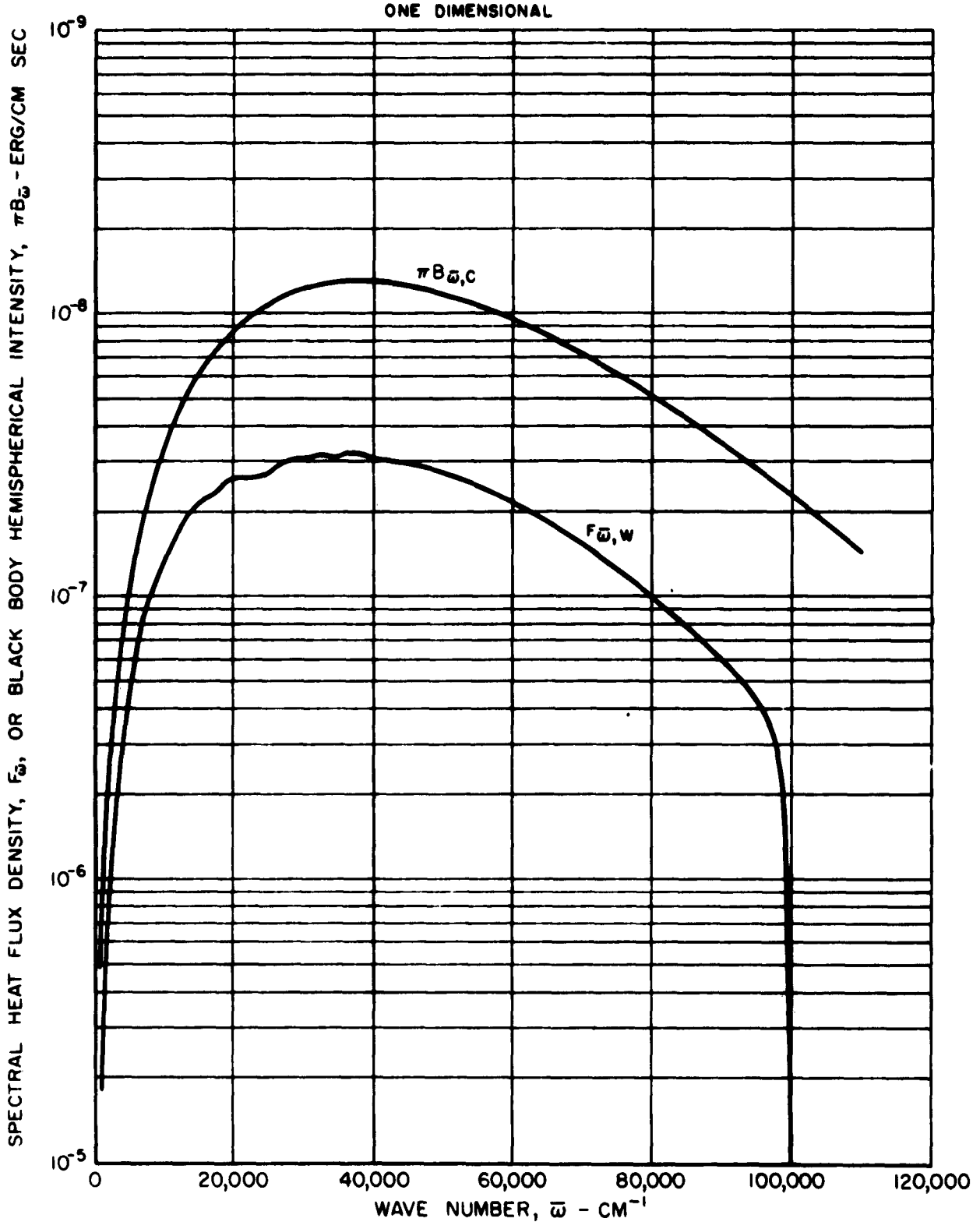

M-1492-1

FIG. 11

NET ENERGY LOSS FOR A TYPICAL CASE
HYDROGEN + GREY GAS

P = 100 ATM

D = 30.48 CM = 1 FT

T_C = 19,444 K = 35,000 R

T_W = 2222.2 K = 4000 R

ONE DIMENSIONAL